This version of the manuscript is the final revised one of the published on-line on 16 April 2015:
https://pubs.acs.org/doi/10.1021/acs.molpharmaceut.5b00085

Oleanolic acid-loaded PEGylated PLA and PLGA nanoparticles with enhanced cytotoxic activity against cancer cells

Dede K.W. Man[1], Luca Casettari[2], Marco Cespi[3], Giulia Bonacucina[3], Giovanni F. Palmieri[3], Stephen C.W. Sze[4], George P.H. Leung[1], Jenny K.W. Lam[1] and Philip C.L. Kwok[1]*

[1]Department of Pharmacology & Pharmacy, Li Ka Shing Faculty of Medicine, The University of Hong Kong, Pokfulam, Hong Kong

[2]Department of Biomolecular Sciences, School of Pharmacy, University of Urbino, Piazza Rinascimento, 6, 61029 Urbino (PU), Italy

[3]School of Pharmacy, University of Camerino, via S. Agostino 1, 62032 Camerino, MC, Italy

[4]School of Chinese Medicine, Li Ka Shing Faculty of Medicine, The University of Hong Kong, Pokfulam, Hong Kong

KEYWORDS: nanoparticles, PLGA, PLA, cytotoxicity, oleanolic acid, PEGylation

25 **TABLE OF CONTENTS GRAPHIC**

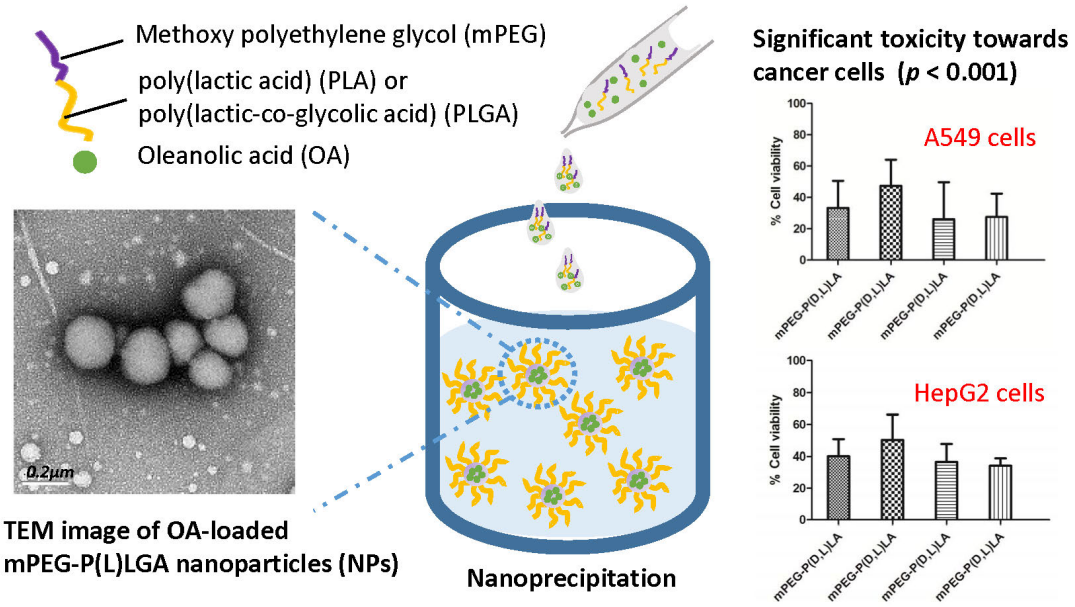

26

27

28

29

30

31

32

33

ABSTRACT

Oleanolic acid (OA) is a natural triterpenoid with anticancer property, but its hydrophobic nature and poor aqueous solubility pose challenges in pharmaceutical formulation development. The present study aimed at developing OA-loaded mPEG-PLGA or mPEG-PLA nanoparticles (NPs) to improve the delivery of OA. The NPs were prepared by nanoprecipitation and their physicochemical properties were characterized. The OA encapsulation efficiency of the NPs was between 40 to 75%. The size of the OA-loaded NPs was around 200-250 nm, which fell within the range required for tumour targeting by means of enhanced permeability and retention (EPR) effect, and the negatively charged NPs remained physically stable for over 20 weeks with no aggregation observed. The OA-loaded NPs produced significant cytotoxic effect through apoptosis in cancer cell lines. Overall, the OA-loaded mPEG-PLGA NPs and mPEG-PLA NPs shared similar physicochemical properties. The former, especially the OA-loaded mPEG-P(D,L)LGA NPs, were more cytotoxic to cancer cells and therefore were more efficient for OA delivery.

INTRODUCTION

Cancer is the leading cause of death worldwide. Current chemotherapeutic agents are inadequate, especially with the increasing number of multidrug resistant cancer. High toxicity of anticancer drugs is another problem associated with the management of cancer. Nanotechnology-based strategies have been proposed to improve the delivery of anticancer drugs [1]. Biodegradable polymer nanoparticles (NPs) can provide a safe alternative to maintain the effective drug concentrations within the therapeutic window for sustainable therapy, leading to the reduction of adverse effects and frequency of administration. To achieve long circulation time, the drug-loaded NPs must be able to escape elimination by the reticuloendothelial system (RES). In order to avoid clearance by phagocytosis, the surfaces of colloidal particles are usually modified by hydrophilic agents, such as polyethylene glycol (PEG), which alter the physicochemical properties of the NPs and consequently the performance of NPs such as drug release profile, biodistribution and pharmacokinetics [2]. Amphiphilic block copolymers consist of both hydrophobic and hydrophilic parts that allow them to self-assemble into core-shell type polymeric micelles, into which hydrophilic as well as hydrophobic drugs can be loaded [3, 4].

PEGylated polyesters such as poly(lactic acid) (PLA) or poly(lactic-co-glycolic acid) (PLGA) have been intensively investigated as drug delivery systems, particularly in the field of oncology. The nanoparticulate formulations of these polymers are developed with the attempt to improve drug delivery by enhancing the aqueous solubility of poorly soluble drugs, protecting them from premature degradation, achieving sustained release while minimizing the toxic effects on normal tissues [5-8]. In addition, NPs without any specific targeting ligand can rely on the enhanced permeability and retention (EPR) effect

to deliver drugs to cancer cells [9]. EPR is a passive targeting strategy to solid tumors mainly based on particle size. Due to the abnormally leaky vasculature found in tumor tissues, NPs that are smaller than the vascular pores within the tumor tissue can deposit and accumulate in the tumor interstitial space and release the loaded drug. Therefore, chemotherapeutic agents encapsulated in NPs can be potentially retained in tumors and released at the target sites in a controlled manner. It has been suggested that NPs with a diameter of 50 to 400 nm could target tumor tissues by EPR [10] although the exact size range is controversial, as size is not the only determinant factor for EPR to occur [9]. Recently, Genexol®-PM, a nanoparticle formulation of paclitaxel, in which the drug is loaded in biodegradable PEG-PLA polymer micelles, has been approved in Korea for the treatment of ovarian and metastasis breast cancer. The formulation is now under Phase IV trial in the USA as a safer alternative to Taxol® [11, 12]. Another PEG-PLA/PEG-PLGA mixed polymer micelle formulation encapsulating doxorubicin that targets prostate-specific membrane antigen is currently in Phase II clinical trial [13].

Traditional Chinese medicines (TCMs) have been frequently studied for the treatment of various types of cancers [14, 15]. Triterpenoid saponins are glycosylated plant secondary metabolites widely existing in food, crops and herbal plants in high content [16]. Among all triterpenoids, pentacyclic triterpenes attract most attention due to their high diversity of structures and biological activities. Their uses as anticancer and anti-HIV agents have been extensively studied [17-20]. Being the most predominant member of pentacyclic triterpenoids, oleanolic acid (OA) [(3β)-3-hydroxyolean-12-en-28-oic acid] (Fig. 1) is widely present in Chinese herbs [21]. OA exhibits many important biological actions, such as anti-inflammatory, anti-nociceptive, antioxidant and anti-diabetic properties [22-24]. It is especially well-known for its hepatoprotective activity [21, 25-27]. Moreover, its anticancer

activity has been extensively demonstrated [28, 29]. However, the clinical application of OA has been limited by its poor aqueous solubility (4.61 μg/ml at 20 °C) and extremely low dissolution rate in the gastrointestinal tract. Hence its oral bioavailability is low [21].

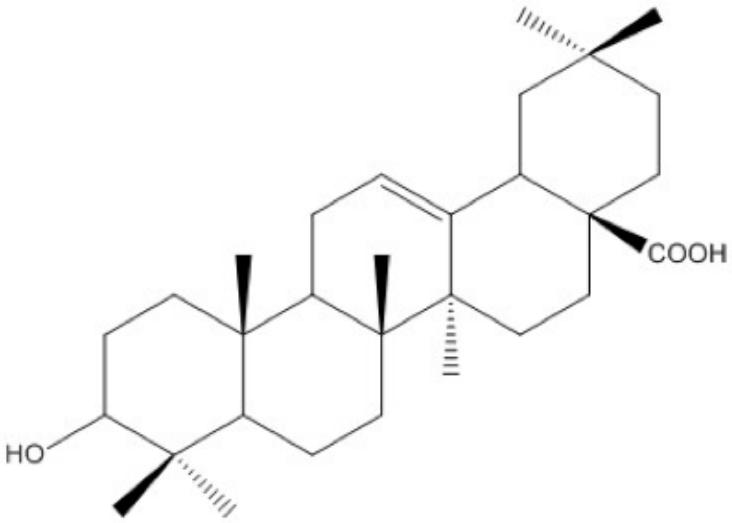

Figure 1. Chemical structure of oleanolic acid (OA).

A number of formulation strategies have been explored to improve the delivery of OA. By formulating OA into a nanosupension, the saturation solubility of OA was successfully increased by almost 550-folds [30]. The encapsulation of OA by lipid NPs was found to improve drug absorption significantly compared to free OA [31]. It was also reported that microemulsions markedly enhanced the oral bioavailability of OA by around five-folds [32]. Anti-tumor activity of OA had also been tested *in vivo* after encapsulation into PEGylated liposomes. Following oral administration in mice, the PEGylated OA liposomes successfully inhibited tumor growth by over 75 % [33]. More recently, an OA-loaded PLGA-TPGS (D-α-tocopheryl polyethylene glycol succinate) delivery system showed exceptional therapeutic effect for liver cancer [34].

The aim of this study was to develop a biodegradable nanoparticulate drug delivery system to enhance the solubility and the cytotoxic effect of OA in cancer cells. Four di-block copolymers, mPEG-P(D,L)LA, mPEG-P(L)LA, mPEG-P(D,L)LGA and mPEG-P(L)LGA, were employed to prepare OA-loaded NPs using nanoprecipitation method [35]. These biodegradable polymers have similar molecular weight (all below 10 kDa) but with different crystallinity and degradation rates (degradation time: P(L)LA>P(D,L)LA>P(L)LGA>P(D,L)LGA) [36]. The physicochemical properties of the NPs were characterized in terms of their size distribution, zeta potential, morphology as well as physical stability. The cytotoxic effect of OA on lung and liver cancer cells was reported previously [37, 38]. To evaluate the cytotoxic effect of OA in our NPs formulation, human lung cancer cell line (A549) and human liver cancer cell line (HepG2) were used. In addition, human bronchial epithelial cell line (BEAS-2B), which is a non-cancer cell line, was also used. The cytotoxic study was carried out by MTT (3-(4, 5-dimethylthiazolyl-2)-2, 5- diphenyltetrazolium bromide) assay. The induced cell death pathway was also investigated.

EXPERIMENTAL SECTION

Materials

Methoxy poly (ethylene glycol) (mPEG) Mw 5 kDa was purchased from Polysciences. DL-lactide, L-lactide and glycolide were kindly donated by PURAC Biochem (Gorinchem, Netherlands). Stannous-2-ethyl-hexanoate was purchased by Sigma-Aldrich (Milan, Italy). Oleanolic acid was a obtained from International Laboratory USA, San Francisco, CA, USA. 3-(4, 5-dimethylthiazolyl-2)-2, 5- diphenyltetrazolium bromide (MTT), acetone, acetonitrile, 85% phosphoric acid, methanol, ethanol and 2-propanol were purchased from Merck (Darmstadt, Germany). Annexin V-FITC apoptosis detection kit (V13242) was obtained from Invitrogen, Life Technologies (USA). Water was of MilliQ grade purified by the Barnstead™ Nanopure™ system (Dubuque, IA). Dulbecco's Modified Eagle Medium (DMEM) and Keratinocyte-SFM (1X) with Bovine Pituitary Extract and EGF Human Recombinant were purchased from Invitrogen (Carlsbad, VA, USA). All other reagents were standard reagent grade or higher and used without further purification.

Synthesis of di-block copolymers

Four different copolymers were synthesized following the ring-opening polymerization (ROP) method: mPEG-P(D,L)LA, mPEG-P(L)LA, mPEG-P(D,L)LGA and mPEG-P(L)LGA. mPEG 5 kDa was added to a schlenk tube and melted at 80°C, under magnetic stirring and nitrogen gas. Lactide and/or glycolide was then added into the flask with increasing temperature to 150°C. Finally, stannous-2-ethyl-hexanoate was added into the mixture, and the reaction was heated at 150°C for 4 h [39]. Dichloromethane was added to the reaction mixture at room temperature, and the viscous solution was poured into cold diethyl ether, under stirring, to precipitate the copolymers. The precipitated material was filtered and put under vacuum to remove any trace of solvents. The obtained powder was

stored at 4°C for further investigations.

Characterization of the di-block copolymers

The synthesized copolymers were characterised by proton nuclear magnetic resonance (^{1}H-NMR) and gel permeation chromatography (GPC). In the NMR study, samples were dissolved in deuterium chloroform ($CDCl_3$) and ^{1}H-NMR spectra were recorded on a Bruker Advance 200 MHz spectrometer. Chemical shift values were reported in parts per million (δ) downfield from the internal standard tetramethylsilane (Me_4Si). For the GPC study, 7.5 mg of copolymers were solubilized into 1.5 ml of tetrahydrofuran (THF) at 40 olution was filtered with a regenerated cellulose syringe filter (0.45 µm pore size) and 7.5 µl of CH_3CN, the flow marker, was added. The analyses were carried out using a high performance liquid chromatography (HPLC) (Agilent 1100 series), equipped with a gel permeation column (TSKGel 2500H_{HR} from Tosoh Bioscience) kept at 35°C and using THF as eluent with a flow rate of 1 ml/min. A calibration standard curve was achieved using a PEG calibration kit (PL2070-01000 by Varian) with molecular weight ranging from 106 to 21,300 Mp. Data were analyzed by the clarity software DATAAPEX (DataApex Ltd, Prague, Czech Republic) [40].

Preparation of polymeric NPs (blank or OA-loaded)

Polymeric NPs were prepared using nanoprecipitation method. 20 mg of a di-block copolymer, mPEG-P(D,L)LA, mPEG-P(L)LA, mPEG-P(D,L)LGA or mPEG-P(L)LGA, was weighed and dissolved in 300 µl of acetone. For OA-loaded NPs, 2 mg of OA was mixed with the copolymer solution. The mixture was sonicated until complete dissolution. The solution was then added drop-wise into 3 ml of water under magnetic stirring. NPs were formed instantaneously and the dispersion was then stirred overnight to allow evaporation of the organic solvent. The NP water dispersion was centrifuged at 13,000

184 rpm for 20 minutes at 4°C to remove free OA. The sedimented NPs were then
185 re-suspended in water and stored at 4°C until use.

186 ***Physicochemical characterization of NPs***

187 The hydrodynamic diameter of the NPs was measured by dynamic light scattering (DLS)
188 (Delsa Nano C Zetasizer, Beckman Coulter, USA). Freshly prepared NPs were diluted in
189 water (5-6 mg/ml of copolymer) to achieve optimal measuring intensity for particle size
190 measurement. The zeta potential of NPs was determined by electrophoretic light scattering
191 in a flow cell (Delsa Nano C Zetasizer, Beckman Coulter, USA). Experimental values
192 presented were the average of three independent preparations. The morphology of NPs
193 was examined using transmission electron microscopy (TEM) (FEI Tecnai G2 20 S-TWIN
194 TEM, Hillsboro, OR). A drop of NP suspension was deposited onto a 400 mesh copper
195 grid with carbon and was laid to dry in air at room temperature. It was then negatively
196 stained with 2% (w/v) uranyl acetate and allowed to dry before measurement.

197 ***Drug loading and encapsulation efficiency***

198 Drug loading (DL) and encapsulation efficiency (EE) of OA-loaded NPs were evaluated
199 with HPLC using the protocol reported by Tong *et al.* with slight modification [41]. 500 µl
200 of the OA-containing NP formulation was centrifuged. The supernatant was discarded and
201 the precipitate was re-dissolved in 200 µl of acetone. The analysis was performed with an
202 Agilent 1260 infinity HPLC system equipped with a photodiode array detector (DAD)
203 scanning the 190-400 nm range. An Agilent Zorbaz Prep-C18 column (5 µm coarse, 250
204 mm x 4.6 mm) was used at 25°C. Samples were injected at 20 µl. An isocratic method was
205 used for separation in which the mobile phase A consisted of 0.5% phosphoric acid and
206 the mobile phase B was acetonitrile. The samples were eluted at mobile phase volumetric
207 ratio 15:85 (A:B) at 1.0 ml/min. The wavelength for OA quantification was 205 nm. OA

concentration was determined with a calibration curve obtained by standard solutions of OA in acetone (5.21-333.3 μg/ml). DL was calculated by the ratio of the amount of drug encapsulated in NPs and the amount of copolymer added. EE was expressed as the ratio between amount of drug loaded and initial amount of drug input.

$$Drug\ Loading\ (\%) = \frac{Amount\ of\ OA\ in\ nanoparticles}{Amount\ of\ copolymer\ added} \times 100$$

$$Encapsulation\ Efficicency\ (\%) = \frac{Amount\ of\ OA\ in\ nanoparticles}{Initial\ amount\ of\ OA} \times 100$$

Cell culture

A549 cells and HepG2 cells were obtained from American Type Culture Collection (Manassas, VA, USA) and BEAS-2B cells were obtained from American Type Culture Collection (Rockville, MD, USA). A549 cells and HepG2 cells were cultured in complete DMEM (Life technologies, USA) supplemented with 10% FBS and 1% antibiotics-antimycotic (Life technologies, USA). BEAS-2B cells were cultured in Keratinocyte-SFM with bovine pituitary extract and epidermal growth factor (EGF) human recombinant. All cell lines were maintained in a 5% CO_2 humidified incubator at 37°C.

Cytotoxicity study

Cells were seeded in sterile 96-well culture plates at a density of 1 x 10^4 cells per well. The cells were incubated for 24 h to allow cell attachment. Polymeric NPs (with or without OA) suspended in either DMEM or K-SFM were added to the cells. The cytotoxic

effect of OA-loaded NPs was evaluated using the MTT cell viability assay after 24, 48 and 72 h of incubation. Samples were discarded from each well and were replaced by MTT solution (0.8 mg/ml in PBS) for 2 h. The precipitated formazan crystals were dissolved in absolute isopropanol and kept at 4°C for 30 min. Absorbance was measured at 595 nm using a microplate reader (Bio-Tek Microplate Reader, VT, USA). Percentage of viable cells was calculated based on the equation shown below in which untreated cells were taken as control with 100% cell viability.

$$Cell\ Viability\ (\%) = \frac{Absorbance\ of\ sample\ wells}{Absorbance\ of\ control\ wells} \times 100$$

The results were expressed as mean values +/- standard deviation of three independent measurements.

Apoptosis assay

A549 cells were seeded into sterile 6-well plates at a density of 1 x 10^5 cells per well and allowed to settle for 24 h. The cells were treated with OA-loaded polymeric NPs at an OA concentration of 100 µg/ml for 24 h. Untreated cells were used as negative control and cells treated with 0.3% hydrogen peroxide for 15 min were used as positive control. The cells were then washed by cold PBS and collected by centrifugation at 1,000 rpm for 5 min. An annexin V-FITC/PI kit was employed to determine the percentage of apoptosis according to the manufacturer's protocol. The cells were analyzed within 15 min by flow cytometry (BD LSR Fortessa Analyzer, New Jersey, USA).

Statistical Analysis

All results are expressed as means ± standard deviation. Statistical analysis was conducted with GraphPad Prism 5 for Windows. Statistical significance was assessed by one-way or two-way analysis of variance (ANOVA) and Bonferroni *post-hoc* tests. Differences were considered statistically significant with $p < 0.05$.

RESULTS

^{1}H-NMR and GPC characterizations of di-block copolymers

Synthesized PEGylated polyesters were characterized by ^{1}H-NMR spectroscopy ($CDCl_3$) and GPC using THF as mobile phase (Table 1). The ^{1}H-NMR spectra (Fig. 2) showed a peak at 5.2 ppm corresponding to the methine lactide proton (single bond CH), a peak at 4.3 ppm for the methylene group of glycolide, a peak at 3.6 ppm for the protons of the repeating units in the polyethylene glycol chain (single bond OCH_2 single bond CH_2), a peak at 3.4 ppm for the protons of the methyl group of the methoxy PEG end, and a peak at 1.5 ppm for the methyl group of the lactide chain (single bond CH_3).

Table 1. Characterization of the diblock copolymers included in the formulations. Polymers were characterized by proton nuclear magnetic resonance (^{1}H-NMR) and gel permeation chromatography (GPC). PDI = polydispersity index.

Copolymers	^{1}H-NMR	GPC		
	M_n (Da)	M_n (Da)	M_w (Da)	PDI
mPEG 5 kDa	5500	6033	6714	1.11
mPEG5kDa -P(L)LA	6500	6771	9837	1.45
mPEG5kDa-P(D,L)LA	6700	7219	9384	1.30
mPEG5kDa -P(L)LGA	6550	6739	9165	1.36
mPEG5kDa -P(D,L)LGA	6600	7075	9850	1.39

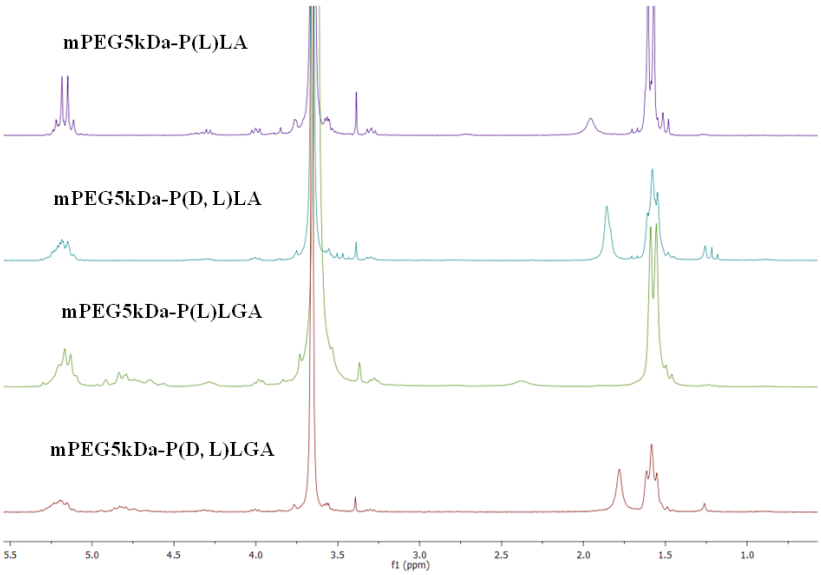

Figure 2. ^{1}H NMR spectra of diblock copolymer. The spectra were measured using a Bruker Advance 200 MHz spectrometer. Chemical shift values were reported in parts per million (δ) downfield from the internal standard tetramethylsilane (Me_4Si).

Particle size distribution and zeta potential (ζ)

The mean diameters of blank NPs were all below 70 nm with similar size distributions (Table 2). After OA was loaded in NPs, particle size increased. All the OA-loaded NPs were in the range of 200 to 250 nm. NPs formed with different copolymers did not show apparent size differences. The polydispersity index (PDI) of all NPs was below 0.3 indicating the relatively narrow size distribution. All the NPs were negatively charged on their surfaces (Table 2). The OA-loaded NPs were more negatively charged than the blank NPs. Overall, the OA-loaded mPEG-PLA NPs were larger in size (240 to 250 nm) with a higher magnitude of zeta potential (-15 to -20 mV) than OA-loaded mPEG-PLGA (200 to 215 nm and -6 to -8 mV for size and zeta potential, respectively).

290 **Table 2. Physicochemical characterizations of nanoparticles (NPs), either blank or**
291 **OA-loaded, prepared by four different types of copolymers.** NPs were suspended in water
292 during measurement. The data were presented as mean ± standard deviation (n = 3). PDI =
293 polydispersity index.

	Copolymer	Diameter (nm)	PDI	Zeta potential (mV)
Blank NPs	mPEG-P(D,L)LA	67.4 ± 6.51	0.18 ± 0.04	-3.7 ± 0.76
	mPEG-P(L)LA	53.4 ± 6.16	0.21 ± 0.03	-10.9 ± 1.31
	mPEG-P(D,L)LGA	62.6 ± 2.72	0.11 ± 0.01	-4.34 ± 0.98
	mPEG-P(L)LGA	39.7 ± 6.72	0.20 ± 0.04	-5.08 ± 1.63
OA-loaded NPs	mPEG-P(D,L)LA/OA	250.2 ± 25.39	0.23 ± 0.03	-15.4 ± 0.77
	mPEG-P(L)LA/OA	239.0 ± 11.62	0.26 ±0.01	-20.1 ± 1.62
	mPEG-P(D,L)LGA/OA	201.5 ± 0.72	0.20 ±0.07	-6.66 ± 0.75
	mPEG-P(L)LGA/OA	216.5 ± 15.10	0.27 ± 0.03	-7.2 ± 0.40

294

295 ***Drug loading and encapsulation efficiency***

296 The drug loading (DL) and encapsulation efficiency (EE) of the four types of OA-loaded
297 NPs were examined (Table 3). The DL% was below 10% for all copolymer systems, with
298 mPEG-P(D,L)LA attaining the highest DL of around 7%. All the systems had an EE of
299 over 40%, with mPEG-P(D,L)LA achieved the highest EE at around 75%, which was
300 significantly higher than that of the two mPEG-PLGA systems, which had EEs of 40 to
301 50%.

302

303 **Table 3. Drug loading (DL) and encapsulation efficiency (EE) of nanoparticles (NPs)**
304 **prepared by four different types of copolymers.** The data were presented as mean ± standard

deviation (n = 3).

OA-loaded NPs	DL %	EE %
mPEG-P(D,L)LA/OA	7.58 ± 0.92	75.8 ± 9.17
mPEG-P(L)LA/OA	6.65 ± 0.42	66.5± 4.21
mPEG-P(D,L)LGA/OA	4.73 ± 0.97	47.3 ± 9.72
mPEG-P(L)LGA/OA	4.08 ± 0.30	40.8 ± 2.97

Morphology study

TEM images of blank (Fig. 3) and OA-loaded NPs (Fig. 4) indicate that the NPs were of a narrow size distribution, all within the nanosize range. The blank NPs were generally spherical in shape with diameters of less than 100 nm. There was an apparent increase in particle size to around 200 nm with the encapsulation of OA. The particle size of NPs observed by TEM was smaller than the hydrodynamic diameter measured by DLS.

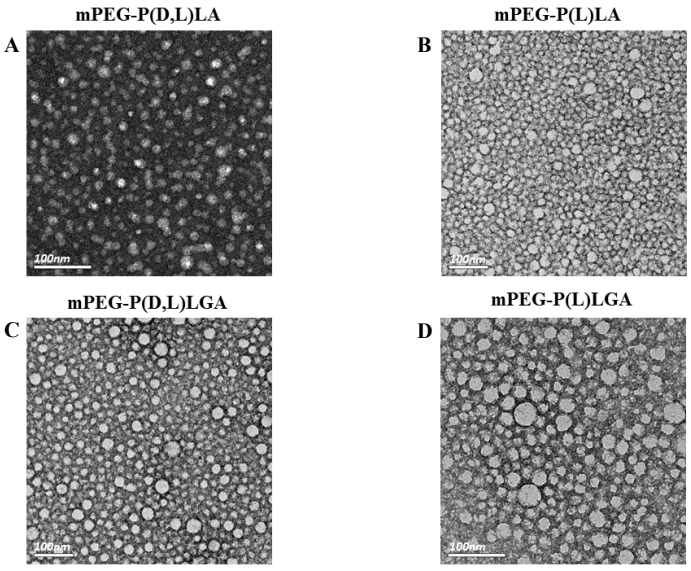

Figure 3. Transmission electron microscopy (TEM) images of blank nanoparticles (NPs). NPs

were prepared with mPEG-P(D,L)LA (A); mPEG-P(L)LA (B); mPEG-P(D,L)LGA (C); mPEG-P(L)LGA (D). The samples were stained with 2% uranyl acetate. (Scale bar = 100 nm)

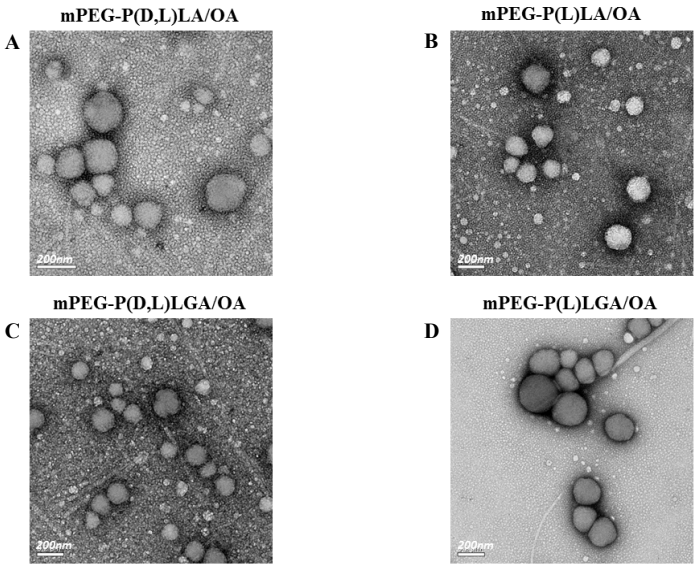

Figure 4. Transmission electron microscopy (TEM) images of oleanolic acid (OA) loaded nanoparticles (NPs). NPs were prepared with mPEG-P(D,L)LA (A); mPEG-P(L)LA (B); mPEG-P(D,L)LGA (C); mPEG-P(L)LGA (D). The samples were stained with 2% uranyl acetate. (Scale bar = 200 nm)

Stability study

The stability of OA-loaded NPs was evaluated by monitoring their particle size distribution after storage at 4°C and 25°C for up to 20 weeks (Table 4). At both storage conditions, all NPs maintained their size below 300 nm with PDI below 0.3 up to 20 weeks. There was no sign of particle aggregation over the storage period.

Table 4. Storage stability of nanoparticles (NPs) prepared by four different types of

copolymers at 4 °C and 25 °C. The data were presented as mean ± standard deviation (n = 3). PDI = polydispersity index.

Copolymer	Week	4 °C storage		25°C storage	
		Diameter (nm)	PDI	Diameter (nm)	PDI
mPEG-P(D,L)LA/OA	1	221.1 ± 4.96	0.18 ± 0.01	247.9 ± 3.54	0.18 ± 0.05
	4	237.9 ± 15.2	0.20 ± 0.02	217.4 ± 0.49	0.10 ± 0.04
	20	217.9 ± 8.47	0.07 ± 0.02	222.2 ± 1.34	0.11 ± 0.00
mPEG-P(L)LA/OA	1	237.0 ± 4.29	0.18 ± 0.01	244.8 ± 1.45	0.20 ± 0.04
	4	190.1 ± 5.59	0.12 ± 0.08	217.2 ±2.03	0.13 ± 0.03
	20	217.0 ± 2.53	0.20 ± 0.06	208.0 ± 2.65	0.15 ± 0.03
mPEG-P(D,L)LGA/OA	1	233.8 ± 3.11	0.15 ± 0.04	213.6 ± 2.06	0.14 ± 0.06
	4	189.6 ± 12.9	0.13 ± 0.05	205.1 ± 2.31	0.10 ± 0.06
	20	182.1 ± 11.2	0.13 ± 0.06	192.0 ± 2.53	0.07 ± 0.02
mPEG-P(L)LGA/OA	1	191.2 ± 4.91	0.16 ± 0.03	205.6 ± 4.50	0.17 ± 0.06
	4	208.8 ± 2.37	0.13 ± 0.01	208.1 ± 9.66	0.18 ± 0.03
	20	180.8 ± 14.2	0.09 ± 0.04	173.7 ± 1.44	0.08 ± 0.00

Cytotoxicity study

Both blank and OA-loaded NPs were tested for their cytotoxic effect on two cancer cell lines, A549 cells (Fig. 5) and HepG2 cells (Fig. 6), and a non-cancer cell line BEAS-2B cells (Fig. 7) by MTT assay. Blank NPs were tested to examine whether or not the polymeric carriers showed any cytotoxic effects. The maximum concentrations of polymers studied were equivalent to the concentrations of polymers used to encapsulate the maximum dose of OA. Cytotoxicity was detected for the blank NPs at high NP concentrations after long incubation time for the two cancer cell lines, and the effect was less prominent on BEAS-2B cells. All the OA-loaded NPs displayed cytotoxicity on both

A549 and HepG2 cells in a time- and concentration-dependent manner. Again, the cytotoxic effect of OA-loaded NPs was less prominent on BEAS-2B cells. The mPEG-PLGA systems were generally more cytotoxic than the mPEG-PLA systems. All of the OA-loaded systems managed to decrease the viability of the cancer cells significantly within 48 h at OA concentration of 40 μg/ml and above. In general, OA-loaded NPs were more cytotoxic to A549 cells than to HepG2 cells. mPEG-P(D,L)LGA/OA NPs were the most cytotoxic, as the cell viability in both cancer cells was lower than that for other systems after the cells were treated with the same OA concentrations. Free OA was also evaluated for their cytotoxic effect in all three cell lines (Fig. 8). The OA was dissolved in the respective cell culture medium. Due to the limitation of the solubility of OA, up to 7.17 μg/ml (on A549 and HepG2 cells) and 3.27 μg/ml (on BEAS-2B cells) of OA, which were the saturated solubility of OA in the culture media, were tested. With respect to the cytotoxic effect on cancer cells by the OA-loaded NPs, the reduction using free OA was less prominent.

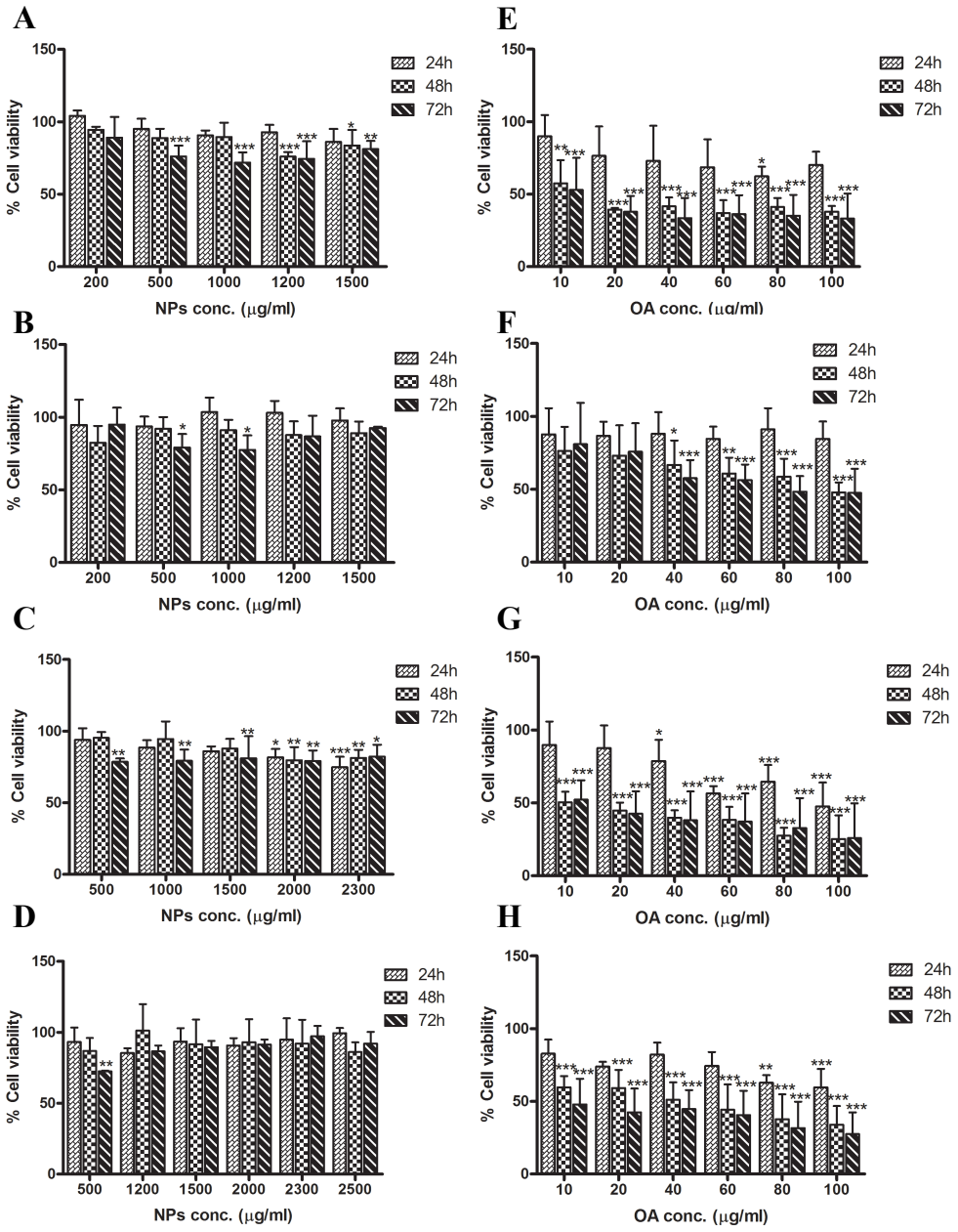

364

365 **Figure 5. Cytotoxicity study of polymeric nanoparticles (NPs) on A549 cells.** The cells were
366 incubated with the blank NPs (A, B, C, D) or OA-loaded NPs (E, F, G, H) of various
367 concentrations for 24 h, 48 h and 72 h before MTT assay was carried out. NPs were prepared with
368 mPEG-P(D,L)LA (A, E); mPEG-P(L)LA (B, F); mPEG-P(D,L)LGA (C, G); mPEG-P(L)LGA (D,
369 H). Data were presented as mean ± standard deviation (n=3). Significant difference was
370 determined by two-way ANOVA analysis, compared to the untreated control. *$p<0.05$, **$p<0.01$,
371 ***$p<0.001$.

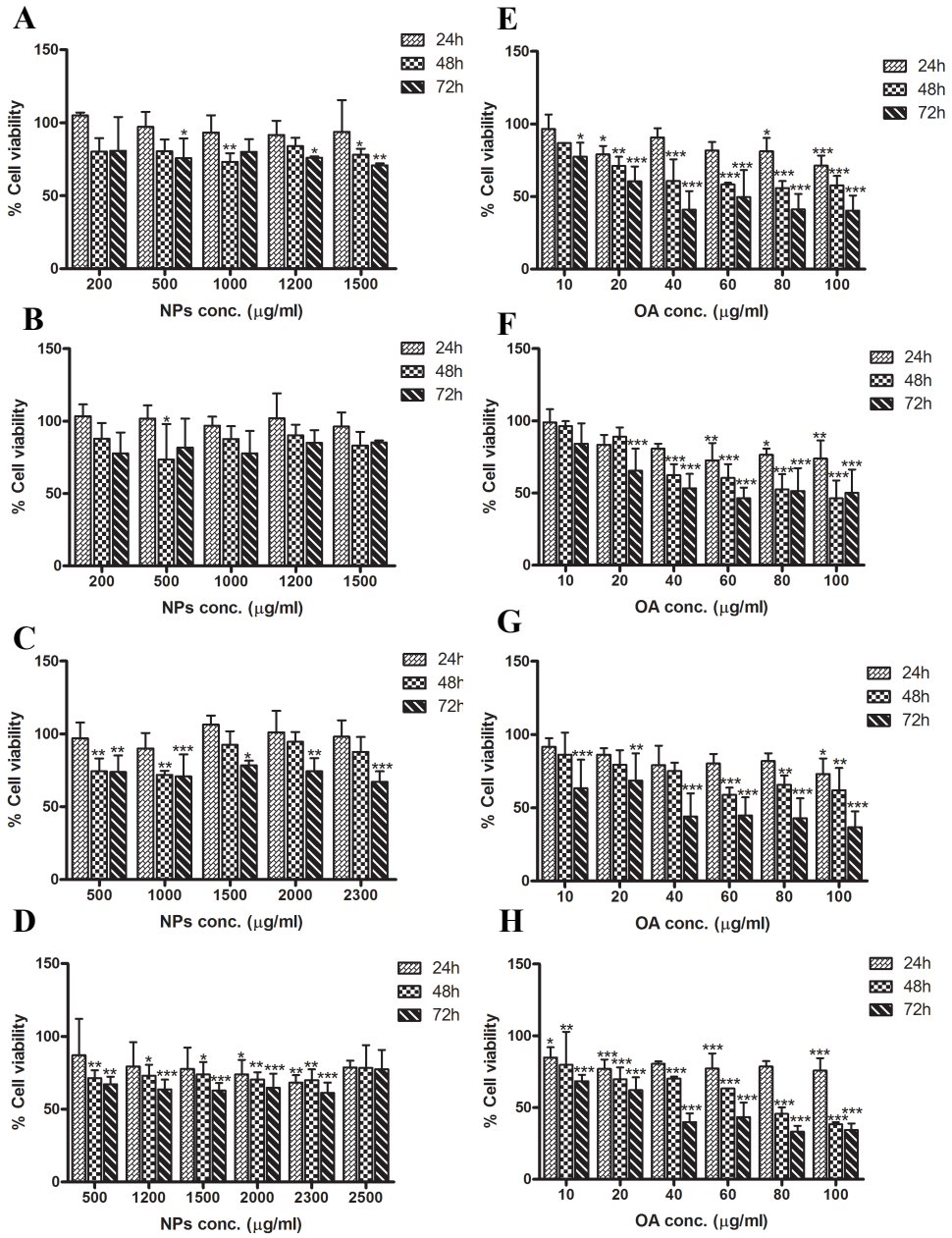

372

373 **Figure 6. Cytotoxicity study of polymeric nanoparticles (NPs) on HepG2 cells.** The cells were
374 incubated with the blank NPs (A, B, C, D) or OA-loaded NPs (E, F, G, H) of various
375 concentrations for 24 h, 48 h and 72 h before MTT assay was carried out. NPs were prepared with
376 mPEG-P(D,L)LA (A, E); mPEG-P(L)LA (B, F); mPEG-P(D,L)LGA (C, G); mPEG-P(L)LGA (D,
377 H). Data were presented as mean ± standard deviation (n=3). Significant difference was
378 determined by two-way ANOVA analysis, compared to the untreated control. *$p<0.05$, **$p<0.01$,
379 ***$p<0.001$.

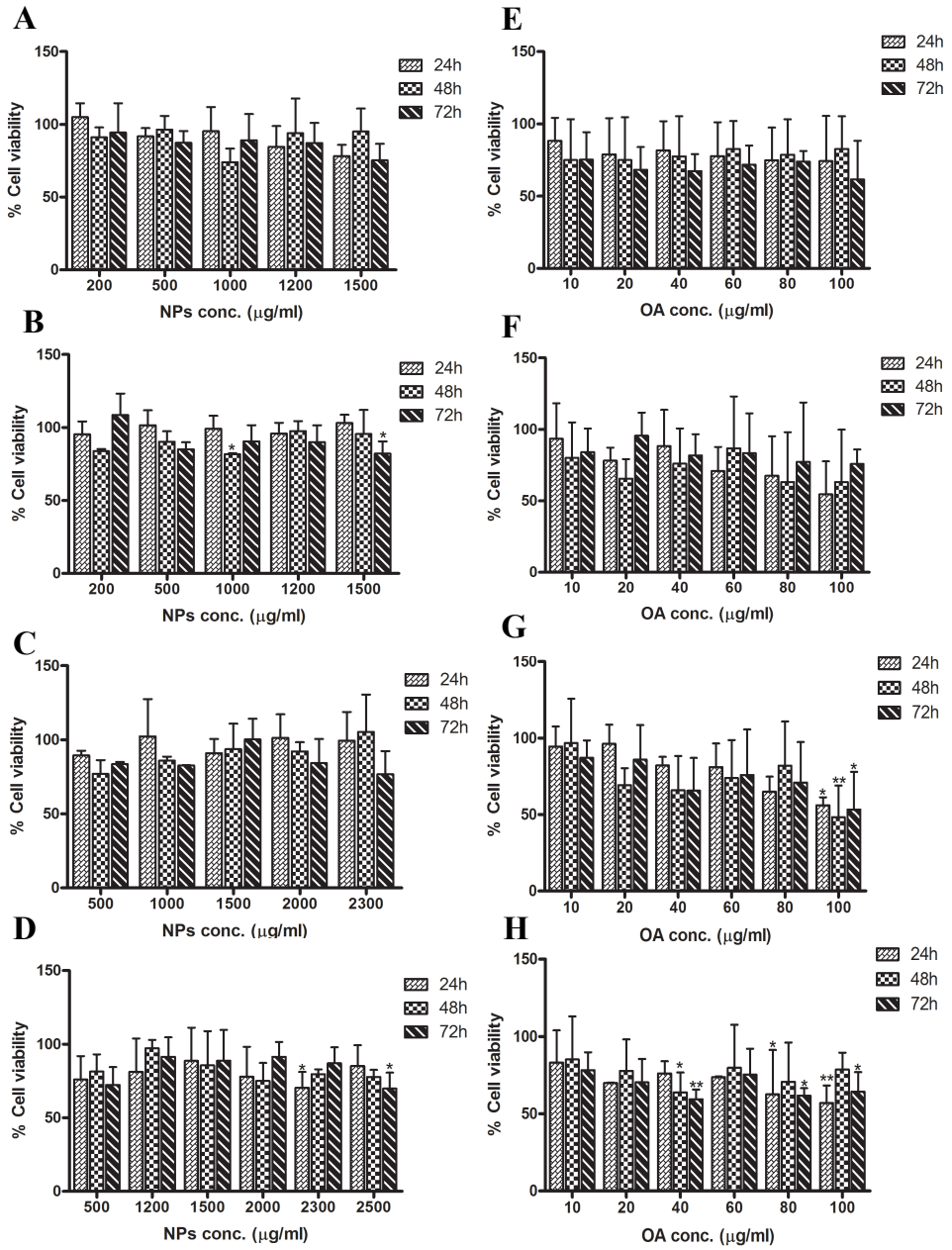

380

381 **Figure 7. Cytotoxicity study of polymeric nanoparticles (NPs) on BEAS-2B cells.** The cells
382 were incubated with the blank NPs (A, B, C, D) or OA-loaded NPs (E, F, G, H) of various
383 concentrations for 24 h, 48 h and 72 h before MTT assay was carried out. NPs were prepared with
384 mPEG-P(D,L)LA (A, E); mPEG-P(L)LA (B, F); mPEG-P(D,L)LGA (C, G); mPEG-P(L)LGA (D,
385 H). Data were presented as mean ± standard deviation (n=3). Significant difference was
386 determined by two-way ANOVA analysis, compared to the untreated control. *$p<0.05$, **$p<0.01$,
387 ***$p<0.001$.

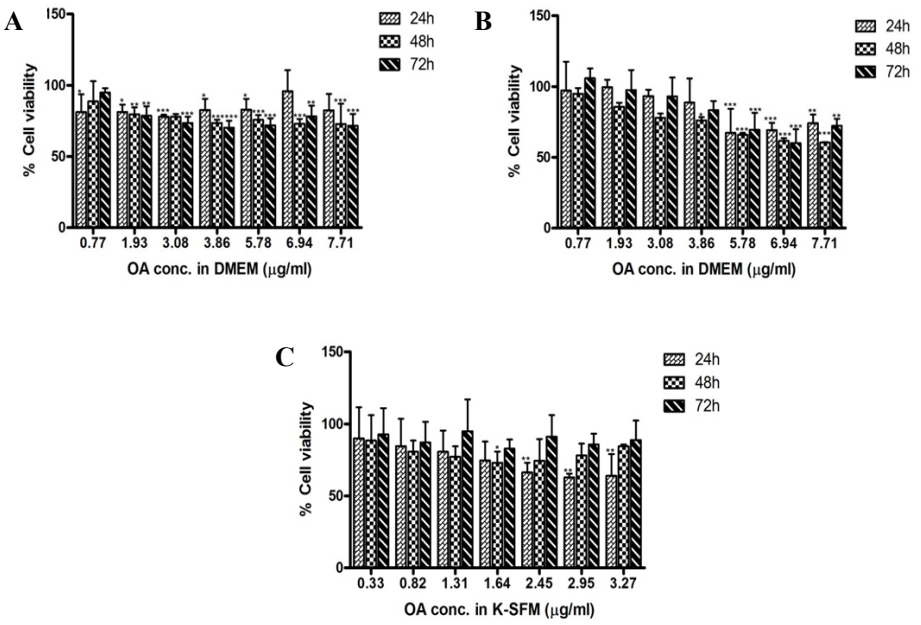

Figure 8. Cytotoxicity study of oleanolic acid (OA) on various cell lines. The cells were incubated with OA dissolved culture medium at various concentrations on A549 cells (A); HepG2 cells (B); BEAS-2B cells (C) for 24 h, 48 h and 72 h before MTT assay was carried out. Data were presented as mean ± standard deviation (n=3). Significant difference was determined by two-way ANOVA analysis, compared to the untreated control. *p<0.05, **p<0.01, ***p<0.001.

Apoptosis assay

In the apoptosis study by flow cytometry (Fig. 9), Q1 represents cell samples that underwent necrosis. None of the OA-loaded NP systems caused necrosis as the signal of the cells were not shown in Q1 for all the NP-treated samples. Normal live cells lied in Q3 as no specific binding occurred on their plasma membrane, indicated by the negative control. The majority of the OA-loaded NPs treated samples gave signals in either Q2 or Q4. Early apoptotic cells were characterized by the phosphatidyl serine residues

externalized from the inner membrane of the cells. Annexin V, a phospholipid binding protein, has a high affinity towards the phosphatidyl serine residues of cells during their early stage of apoptosis. This population of early apoptotic cells was located in Q4 where the FITC signal dominated. For late apoptotic cells, their membranes were damaged, allowing the permeation of both propidium iodide (PI) and annexin V, therefore their signals were shown in Q2. Both early and late apoptosis were observed in cells after 24 h exposure to the OA-loaded NPs. Treatment with mPEG-P(D,L)LGA/OA NPs led to around 70% and 30% of cells in early and late apoptosis, respectively, while treatment with mPEG-P(L)LGA/OA NPs resulted in around 99% of late apoptotic cells. Although relatively higher percentage of viable cells were found after treatment with mPEG-P(D,L)LA/OA and mPEG-P(L)LA/OA NPs, the percentage of early apoptotic cells was found to be between 75% to 85%. These data suggested that apoptotic induced cell death pathway was responsible for the cytotoxic effect on A549 cell using the OA-loaded delivery systems.

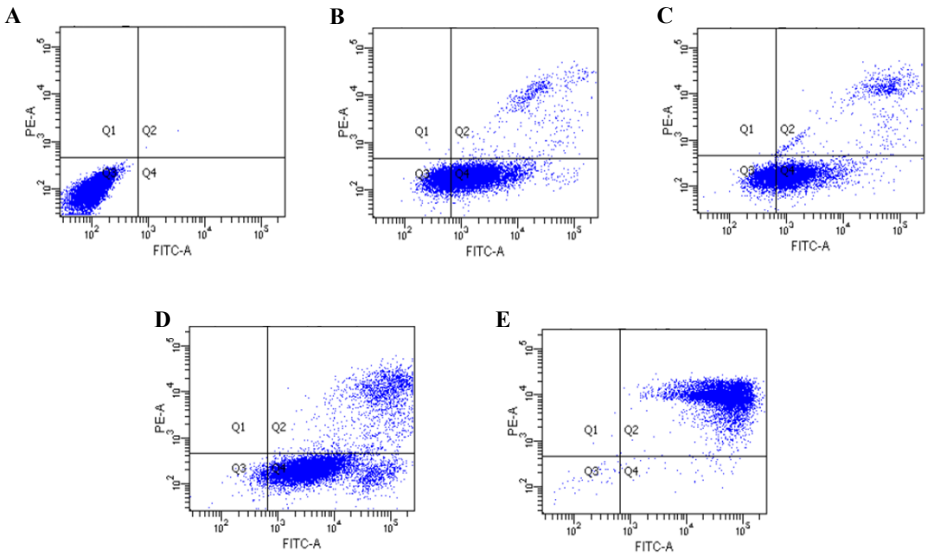

420

421 **Figure 9. Apoptosis assay of oleanolic acid (OA) loaded nanoparticles (NPs) on A549 cells by**
422 **flow cytometry analysis.** Untreated cells were served as control (A). The cells were treated with
423 100 µg/ml OA-loaded NPs prepared with mPEG-P(D,L)LA (B); mPEG-P(L)LA (C);
424 mPEG-P(D,L)LGA (D); mPEG-P(L)LGA (E). Q1 indicates necrotic cells; Q2 indicates late
425 apoptotic cells; Q3 indicates normal healthy cells; Q4 indicates early apoptotic cells.

426

DISCUSSION

OA has shown promising anti-tumor activity in many studies. However, its poor water solubility renders it difficult to be formulated. To address this problem, diblock copolymers mPEG-PLA and mPEG-PLGA were used to prepare NPs in which OA was encapsulated. Their physicochemical properties as well as their efficacies as potential cancer therapeutics were evaluated in this study. The performance of polymeric NPs as drug delivery systems is influenced by a number of parameters, including polymer components, surface modification, size and surface charge of NPs, method of preparation and the properties of the encapsulated drug. PLA and PLGA are hydrophobic, biocompatible and biodegradable polymers that have been widely studied as drug delivery system. Hydrolysis of these polymers leads to metabolite monomers, lactic acid and/or glycolic acid, which are easily metabolized by the body. They are regarded as safe polymers and have been approved by the FDA for clinical applications [42]. In general, PLGA is more commonly used than PLA due to the faster degradation rate. mPEG is a hydrophilic polymer which is frequently used to modify the surface properties of NPs in order to reduce their adsorption with various components in the blood. This surface modification increases the serum stability of NPs and prolongs their circulation half-life [43]. It has been demonstrated that the incorporation of PEG could increase the blood circulation half-life of NPs by several orders of magnitude [44]. In this study, the molecular weight of mPEG block of all the four copolymers was kept constant at 5 kDa, while the hydrophobic block varied between 1.0 and 1.2 kDa (considering ^{1}H-NMR). The selection of 5 kDa mPEG in our delivery systems was based on previous study which reported that NPs containing mPEG 5 kDa was superior to mPEG 2 kDa in delivering chemotherapeutics in terms of their anticancer activity and drug release profile [45].

The size of the four OA-loaded NPs was around 200 to 250 nm, which were comparable to that of similar polymeric NPs reported in the literature [46, 47]. In nanoprecipitation method, OA and the copolymers were dissolved in a common solvent followed by introduction of the solution into a continuously stirring aqueous phase. The hydrophobic segments were precipitated immediately, leading to the spontaneous incorporation of OA into the core of NPs. The whole process is driven by a 'solvent shifting' mechanism [10]. Through this mechanism, drug-loaded NPs are generated when solvent and anti-solvent are mixed together. Due to the intrinsic miscibility, the solvent shifts away from the solute into the anti-solvent; at the same time, the anti-solvent shifts in. Finally, the solutes become supersaturated and precipitate out in the liquid mixture. The PLA and PLGA segments precipitated with the OA in the core while mPEG chains oriented towards the aqueous phase patched over the NP surface to minimize self-aggregation. Apart from being a simple, fast and reproducible method, nanoprecipitation is also economic and can be scaled up to large volume production.

Particle size is highly associated with cellular uptake by endocytosis. NPs with size close to 200 nm generally exhibit higher cellular uptake efficiency [46]. The size of our OA-loaded NPs was around 200-250 nm, suggesting the particles might facilitate cellular uptake in a similar manner. In addition, the size of NPs (<250 nm) fell within the range reported to be favourable in targeting tumors by means of EPR effect [10, 48]. The narrow size distribution of all NPs indicated that the size distribution was quite uniform. The size of NPs illustrated in the TEM images was much smaller than that measured by DLS, a common phenomenon observed in amphiphilic NPs [49, 50]. The measurement of the

475 hydrodynamic size was in a hydrated state in which the NPs were thoroughly swelled,
476 especially with the presence of hydrophilic mPEG on the particle surface, while the TEM
477 images were taken in vacuum with the NPs in the dried state.

478

479 Zeta potential is another critical parameter which determines colloidal stability and the
480 interactions between NPs and plasma components or cell membrane. PLA and PLGA NPs
481 are negatively charged [42]. The PEGylated PLA or PLGA NPs usually possess lower
482 negative charges than the non-PEGylated counterparts, as reported in the literature [51]. This
483 is expected as the hydrophilic mPEG normally form the corona on the surface of NPs,
484 conferring 'stealth' properties which shield the surface charge of the NPs. The magnitude
485 of zeta potential displayed by the OA-loaded mPEG-PLA NPs was higher than that of the
486 OA-loaded mPEG-PLGA NPs. Aggregation occurs relatively easily with NPs of zeta
487 potential close to neutral, ranging from -15mV to +15mV [52]. The zeta potential of
488 OA-loaded mPEG-PLA NPs was above this range, whereas that of OA-loaded
489 mPEG-PLGA NPs was closer to neutral, suggesting that the mPEG-PLA systems were
490 more effective in maintaining colloidal stability. Nevertheless, the stability study indicated
491 that after 20 weeks of storage in either 4 °C or 25 °C, there was no apparent increase in
492 particle size, indicating that all the NPs formulations were stable.

493

494 A good NP drug delivery system should have a high EE, which is the amount of loaded
495 drug relative to the total amount of drug used for the formulation. In our OA-loaded NPs,
496 EE was in the range of 40 – 75%, which was considered to be reasonable and was
497 comparable to other OA-encapsulated nanoparticulate formulations [30, 31]. EE is highly
498 dependent on the physicochemical properties of the loaded drug. Using PLGA-based NPs

as examples, EE of dexamethasone and paclitaxel varied from 6% to 90%, whereas EE of estradiol and xanthones was consistently around 60 – 70% [36, 42].

The cytotoxicity of OA-loaded NPs was examined by MTT assay. Cell viability was greatly reduced through the exposure of OA-loaded NP formulations to the two cancer cell lines, and the NPs were significantly less cytotoxic to the non-cancer cells. The cytotoxic effect of OA on lung and liver cancer cells has been reported previously [37, 38]. It has been demonstrated that OA could suppress the growth of non-small cell lung cancer cell lines while inducing apoptosis and down-regulating VEGF in these cells [53]. Also, OA is renowned for its hepatoprotectivity as a traditional Chinese medicine. It has shown appreciable cytotoxicity on HepG2 cells [54]. The cytotoxic effect of OA-loaded NPs was time and concentration-dependent, and the effect was sustained for 72 h, possibly through the controlled release of OA by both drug diffusion and polymer degradation [55]. The activity of OA was reported to be cell line-dependent, probably due to the different intrinsic sensitivity of the cells. A screening MTT cytotoxicity study of OA was performed by Hao et al. on various cell lines, with DMSO used as solvents [29]. The result showed that OA has the highest activity against A549 cells with an IC_{50} around 450-fold lower than that of HepG2 cells [54]. Our cytotoxicity findings also demonstrated cell line–dependence of OA, but to a much lesser extent. The reduction of cell viability of both cell lines was comparable with the OA-loaded NP system. The increased solubility of OA might be a possible explanation for this observation. Various studies have been performed to demonstrate the ability of NP encapsulation to enhance solubility of OA [56]. Encapsulation of OA by liposomes was investigated and enhanced antitumor activity was displayed on HeLa cells with respect to free OA [57]. Sustained release was observed using OA-loaded nanocapsules, and the drug release was almost seven times slower than that of free OA [58].

Since the solubility of OA is below 5 μg/ml, our NP formulations could greatly enhance the solubility to allow the delivery of OA at 100 μg/ml in aqueous media, indicating the great potential of these polymeric NP systems as drug delivery vehicles.

All four NP formulations were able to reduce A549 cell viability to below 50% after 48 h, reflecting the potential capability of this OA delivery system to be employed in cancer treatment. Although mPEG-PLA/OA had a higher EE, mPEG-PLGA/OA NPs were in general more cytotoxic to cancer cells. This could be due to the differences in surface charge and polymer degradation rate between these two systems. Although both types of NPs were negatively charged, the surface charges of the mPEG-PLGA/OA NPs were closer to neutral, which reduced the electrostatic repulsion from the anionic plasma membrane, leading to better cell internalization. In addition, the difference in degradation rate of the copolymers might also contribute to this observation. PLGA is degraded faster than PLA in general. Consequently, polymer degradation provided the dominant release mechanism of this OA-loaded delivery system, and the faster degradation rate may lead to larger amounts of drug released and therefore higher cytotoxic effects. For mPEG-PLA formulations, the cytotoxic effect of OA-loaded NPs formed with D,L-configuration copolymers was higher than that of the L-configuration counterparts. This could also be explained by the difference in cellular uptake efficiency. Garofalo et al. reported that mPEG-P(L)LA NPs were aggregated outside the cells while mPEG-(D,L)PLA NPs were clearly internalized into the cells, as observed by flow cytometry [59]. Thus, mPEG-(D,L)PLA NPs might facilitate cellular uptake, and resulted in higher cytotoxic activity.

548 The apoptosis assay showed that A549 cells underwent apoptosis after exposure to
549 OA-loaded NP formulations at 100 μg/ml for 24 h. This was consistent with the results
550 obtained from the apoptosis assay treating U14 cervical carcinoma cells with OA-loaded
551 PEGylated liposomes [33]. Furthermore, Li et al. performed a comprehensive apoptosis
552 study of OA, showing that OA could up-regulate the expression level of the pro-apoptotic
553 *bax* gene [60]. Moreover, the activity of caspase-9 and capase-3 was also increased through
554 OA treatment, indicating the induced apoptosis was via the mitochondria-dependent
555 pathway. In this study, higher apoptotic percentage was found in mPEG-PLGA/OA NPs,
556 which corresponded to the higher cytotoxic effect on cancer cells. Furthermore, the
557 mPEG-PLGA/OA NPs, especially mPEG-P(L)LGA/OA system, caused a higher number
558 of cells at late apoptosis. This again could be explained by the differences in polymer
559 degradation rate. PLGA was degraded at a faster rate which allowed earlier release of OA
560 inside the treated cells, and hence caused late apoptosis compared to mPEG-PLA/OA
561 systems which caused primarily early apoptosis. Although mPEG-PLA had higher EE of
562 OA than mPEG-PLGA, the physicochemical properties including particle size, stability
563 and morphology of the NPs were similar between the two types of copolymers.
564 mPEG-PLGA/OA, especially mPEG-P(D,L)-PLGA/OA NPs, were more cytotoxic to
565 cancer cells, and was therefore a more efficient nanoparticulate system for OA delivery.
566 Overall, the cytotoxic effects on A549 and HepG2 cancer cell lines were believed to be
567 due to the enhancement of OA solubility through nanoprecipitation, which produced
568 OA-loaded NPs with high EE together with other desirable features facilitating cellular
569 uptake.

570

571 **CONCLUSIONS**

In this study, hydrophobic OA was efficiently encapsulated in mPEG-PLA and mPEG-PLGA NPs as nano-formulations for cancer therapy. The size of OA-loaded NPs fell within the range for possible tumor targeting through EPR, and the NPs remained physically stable for at least 20 weeks. All our OA-loaded NPs system produced significant cytotoxic effects through apoptosis on cancer cell lines. In general, the NPs formed by mPEG-PLGA and mPEG-PLA had similar physicochemical properties, but the OA-loaded mPEG-PLGA NPs, especially mPEG-P(D,L)LGA, were more cytotoxic to cancer cells and was therefore considered to be a more efficient system for OA delivery. With further investigation, these NP systems have high potentials to be developed into an effective anticancer delivery platform for cancer chemotherapy.

AUTHOR INFORMATION

Corresponding author

* Department of Pharmacology & Pharmacy, Li Ka Shing Faculty of Medicine, The University of Hong Kong, Pokfulam, 21 Sassoon Road, Hong Kong.

Tel: +852 3917 9599; Fax: + 852 2817 0859; Email: **jkwlam@hku.hk**

ACKNOWLEDGEMENTS

The authors thank PURAC Biochem (Netherland), for the generous donation of L-lactide (Purasorb L), D,L-lactide (PURASORB DL) and glycolide (PURASORB G). Professor Henry H Y Tong of The School of Health Sciences, Macao Polytechnic Institute, Macao SAR, is thanked for donating the raw oleanolic acid. The authors thank Faculty Core

Facility, LKS Faculty of Medicine, The University of Hong Kong for the assistance of the flow cytometry experiments.

ABBREVIATIONS

DL, drug loading; DLS, dynamic light scattering; EE, encapsulation efficiency; EPR, enhanced permeability and retention; GPC, gel permeation chromatography; ^{1}H-NMR, proton nuclear magnetic resonance; HPLC, high performance liquid chromatography; mPEG, methoxy poly(ethylene glycol); MTT, 3-(4, 5-dimethylthiazolyl-2)-2, 5-diphenyltetrazolium bromide; PEG, poly(ethylene glycol); PLA, poly(lactic acid); PLGA, poly(lactic-co-glycolic acid); NP, nanoparticle; OA, oleanolic acid; RES, reticuloendothelial system; ROP, ring-opening polymerization; TCMs, traditional Chinese medicines; TEM, transmission electron microscopy; THF, tetrahydrofuran

REFERENCES

1. Dong, Y.; Feng, S. S. In vitro and in vivo evaluation of methoxy polyethylene glycol-polylactide (MPEG-PLA) nanoparticles for small-molecule drug chemotherapy. *Biomaterials* **2007,** *28*, (28), 4154-60.

2. Sant, S.; Poulin, S.; Hildgen, P. Effect of polymer architecture on surface properties, plasma protein adsorption, and cellular interactions of pegylated nanoparticles. *Journal of biomedical materials research. Part A* **2008,** *87*, (4), 885-95.

618 3. Kataoka, K.; Harada, A.; Nagasaki, Y. Block copolymer micelles for drug delivery:
619 design, characterization and biological significance. *Advanced drug delivery reviews* **2001,**
620 *47*, (1), 113-31.
621 4. Rosler, A.; Vandermeulen, G. W.; Klok, H. A. Advanced drug delivery devices via
622 self-assembly of amphiphilic block copolymers. *Advanced drug delivery reviews* **2001,** *53*,
623 (1), 95-108.
624 5. Anand, P.; Nair, H. B.; Sung, B.; Kunnumakkara, A. B.; Yadav, V. R.; Tekmal, R. R.;
625 Aggarwal, B. B. Design of curcumin-loaded PLGA nanoparticles formulation with
626 enhanced cellular uptake, and increased bioactivity in vitro and superior bioavailability in
627 vivo. *Biochemical pharmacology* **2010,** *79*, (3), 330-8.
628 6. Danhier, F.; Lecouturier, N.; Vroman, B.; Jerome, C.; Marchand-Brynaert, J.; Feron,
629 O.; Preat, V. Paclitaxel-loaded PEGylated PLGA-based nanoparticles: in vitro and in
630 vivo evaluation. *Journal of controlled release : official journal of the Controlled Release*
631 *Society* **2009,** *133*, (1), 11-7.
632 7. Ong, B. Y.; Ranganath, S. H.; Lee, L. Y.; Lu, F.; Lee, H. S.; Sahinidis, N. V.; Wang, C.
633 H. Paclitaxel delivery from PLGA foams for controlled release in post-surgical
634 chemotherapy against glioblastoma multiforme. *Biomaterials* **2009,** *30*, (18), 3189-96.
635 8. Li, D.; Sun, H.; Ding, J.; Tang, Z.; Zhang, Y.; Xu, W.; Zhuang, X.; Chen, X.
636 Polymeric topology and composition constrained polyether-polyester micelles for
637 directional antitumor drug delivery. *Acta biomaterialia* **2013,** *9*, (11), 8875-84.
638 9. Maeda, H.; Nakamura, H.; Fang, J. The EPR effect for macromolecular drug
639 delivery to solid tumors: Improvement of tumor uptake, lowering of systemic toxicity, and
640 distinct tumor imaging in vivo. *Advanced drug delivery reviews* **2013,** *65*, (1), 71-9.
641 10. Zhu, Z. Effects of amphiphilic diblock copolymer on drug nanoparticle formation
642 and stability. *Biomaterials* **2013,** *34*, (38), 10238-48.

643 11. Lee, K. S.; Chung, H. C.; Im, S. A.; Park, Y. H.; Kim, C. S.; Kim, S. B.; Rha, S. Y.;
644 Lee, M. Y.; Ro, J. Multicenter phase II trial of Genexol-PM, a Cremophor-free,
645 polymeric micelle formulation of paclitaxel, in patients with metastatic breast cancer.
646 *Breast cancer research and treatment* **2008,** *108*, (2), 241-50.
647 12. Lin, L. Y.; Karwa, A.; Kostelc, J. G.; Lee, N. S.; Dorshow, R. B.; Wooley, K. L.
648 Paclitaxel-loaded SCK nanoparticles: an investigation of loading capacity and cell killing
649 abilities in vitro. *Molecular pharmaceutics* **2012,** *9*, (8), 2248-55.
650 13. Hrkach, J.; Von Hoff, D.; Mukkaram Ali, M.; Andrianova, E.; Auer, J.; Campbell, T.;
651 De Witt, D.; Figa, M.; Figueiredo, M.; Horhota, A.; Low, S.; McDonnell, K.; Peeke, E.;
652 Retnarajan, B.; Sabnis, A.; Schnipper, E.; Song, J. J.; Song, Y. H.; Summa, J.; Tompsett,
653 D.; Troiano, G.; Van Geen Hoven, T.; Wright, J.; LoRusso, P.; Kantoff, P. W.; Bander, N.
654 H.; Sweeney, C.; Farokhzad, O. C.; Langer, R.; Zale, S. Preclinical development and
655 clinical translation of a PSMA-targeted docetaxel nanoparticle with a differentiated
656 pharmacological profile. *Science translational medicine* **2012,** *4*, (128), 128ra39.
657 14. Wang, C. Y.; Bai, X. Y.; Wang, C. H. Traditional Chinese medicine: a treasured
658 natural resource of anticancer drug research and development. *The American journal of*
659 *Chinese medicine* **2014,** *42*, (3), 543-59.
660 15. Hsiao, W. L.; Liu, L. The role of traditional Chinese herbal medicines in cancer
661 therapy--from TCM theory to mechanistic insights. *Planta medica* **2010,** *76*, (11),
662 1118-31.
663 16. Liu, Q.; Liu, H.; Zhang, L.; Guo, T.; Wang, P.; Geng, M.; Li, Y. Synthesis and
664 antitumor activities of naturally occurring oleanolic acid triterpenoid saponins and their
665 derivatives. *European journal of medicinal chemistry* **2013,** *64*, 1-15.
666 17. Shi, L. S.; Wu, C. H.; Yang, T. C.; Yao, C. W.; Lin, H. C.; Chang, W. L. Cytotoxic
667 effect of triterpenoids from the root bark of Hibiscus syriacus. *Fitoterapia* **2014,** *97*,

668 184-91.
669 18. Kongkum, N.; Tuchinda, P.; Pohmakotr, M.; Reutrakul, V.; Piyachaturawat, P.;
670 Jariyawat, S.; Suksen, K.; Akkarawongsapat, R.; Kasisit, J.; Napaswad, C. Cytotoxic,
671 antitopoisomerase IIalpha, and anti-HIV-1 activities of triterpenoids isolated from leaves
672 and twigs of Gardenia carinata. *Journal of natural products* **2013,** *76*, (4), 530-7.
673 19. Osorio, A. A.; Munoz, A.; Torres-Romero, D.; Bedoya, L. M.; Perestelo, N. R.;
674 Jimenez, I. A.; Alcami, J.; Bazzocchi, I. L. Olean-18-ene triterpenoids from Celastraceae
675 species inhibit HIV replication targeting NF-kB and Sp1 dependent transcription.
676 *European journal of medicinal chemistry* **2012,** *52*, 295-303.
677 20. Liby, K. T.; Yore, M. M.; Sporn, M. B. Triterpenoids and rexinoids as
678 multifunctional agents for the prevention and treatment of cancer. *Nature reviews. Cancer*
679 **2007,** *7*, (5), 357-69.
680 21. Liu, J. Oleanolic acid and ursolic acid: research perspectives. *Journal of*
681 *ethnopharmacology* **2005,** *100*, (1-2), 92-4.
682 22. Wang, X.; Ye, X. L.; Liu, R.; Chen, H. L.; Bai, H.; Liang, X.; Zhang, X. D.; Wang, Z.;
683 Li, W. L.; Hai, C. X. Antioxidant activities of oleanolic acid in vitro: possible role of
684 Nrf2 and MAP kinases. *Chemico-biological interactions* **2010,** *184*, (3), 328-37.
685 23. Martin, R.; Cordova, C.; San Roman, J. A.; Gutierrez, B.; Cachofeiro, V.; Nieto, M. L.
686 Oleanolic acid modulates the immune-inflammatory response in mice with experimental
687 autoimmune myocarditis and protects from cardiac injury. Therapeutic implications for the
688 human disease. *Journal of molecular and cellular cardiology* **2014,** *72*, 250-62.
689 24. Maia, J. L.; Lima-Junior, R. C.; Melo, C. M.; David, J. P.; David, J. M.; Campos, A.
690 R.; Santos, F. A.; Rao, V. S. Oleanolic acid, a pentacyclic triterpene attenuates
691 capsaicin-induced nociception in mice: possible mechanisms. *Pharmacological research :*
692 *the official journal of the Italian Pharmacological Society* **2006,** *54*, (4), 282-6.

693 25. Jeong, H. G. Inhibition of cytochrome P450 2E1 expression by oleanolic acid:
694 hepatoprotective effects against carbon tetrachloride-induced hepatic injury. *Toxicology*
695 *letters* **1999,** *105*, (3), 215-22.
696 26. Liu, J.; Liu, Y.; Parkinson, A.; Klaassen, C. D. Effect of oleanolic acid on hepatic
697 toxicant-activating and detoxifying systems in mice. *The Journal of pharmacology and*
698 *experimental therapeutics* **1995,** *275*, (2), 768-74.
699 27. Pollier, J.; Goossens, A. Oleanolic acid. *Phytochemistry* **2012,** *77*, 10-5.
700 28. Uto, T.; Sakamoto, A.; Tung, N. H.; Fujiki, T.; Kishihara, K.; Oiso, S.; Kariyazono,
701 H.; Morinaga, O.; Shoyama, Y. Anti-Proliferative Activities and Apoptosis Induction by
702 Triterpenes Derived from Eriobotrya japonica in Human Leukemia Cell Lines.
703 *International journal of molecular sciences* **2013,** *14*, (2), 4106-20.
704 29. Hao, J.; Liu, J.; Wen, X.; Sun, H. Synthesis and cytotoxicity evaluation of oleanolic
705 acid derivatives. *Bioorganic & medicinal chemistry letters* **2013,** *23*, (7), 2074-7.
706 30. Li, W.; Das, S.; Ng, K. Y.; Heng, P. W. Formulation, biological and
707 pharmacokinetic studies of sucrose ester-stabilized nanosuspensions of oleanolic Acid.
708 *Pharmaceutical research* **2011,** *28*, (8), 2020-33.
709 31. Zhang, K.; Lv, S.; Li, X.; Feng, Y.; Li, X.; Liu, L.; Li, S.; Li, Y. Preparation,
710 characterization, and in vivo pharmacokinetics of nanostructured lipid carriers loaded with
711 oleanolic acid and gentiopicrin. *International journal of nanomedicine* **2013,** *8*, 3227-39.
712 32. Yang, R.; Huang, X.; Dou, J.; Zhai, G.; Su, L. Self-microemulsifying drug delivery
713 system for improved oral bioavailability of oleanolic acid: design and evaluation.
714 *International journal of nanomedicine* **2013,** *8*, 2917-26.
715 33. Tang, S.; Gao, D.; Zhao, T.; Zhou, J.; Zhao, X. An evaluation of the anti-tumor
716 efficacy of oleanolic acid-loaded PEGylated liposomes. *Nanotechnology* **2013,** *24*, (23),
717 235102.

718 34. Bao, X.; Gao, M.; Xu, H.; Liu, K. X.; Zhang, C. H.; Jiang, N.; Chu, Q. C.; Guan, X.;
719 Tian, Y. A novel oleanolic acid-loaded PLGA-TPGS nanoparticle for liver cancer
720 treatment. *Drug development and industrial pharmacy* **2014**, 1-11.
721 35. Fessi, H.; Puisieux, F.; Devissaguet, J. P.; Ammoury, N.; Benita, S. Nanocapsule
722 Formation by Interfacial Polymer Deposition Following Solvent Displacement.
723 *International journal of pharmaceutics* **1989,** *55*, (1), R1-R4.
724 36. Kumari, A.; Yadav, S. K.; Yadav, S. C. Biodegradable polymeric nanoparticles
725 based drug delivery systems. *Colloids and surfaces. B, Biointerfaces* **2010,** *75*, (1), 1-18.
726 37. Lucio, K. A.; Rocha Gda, G.; Moncao-Ribeiro, L. C.; Fernandes, J.; Takiya, C. M.;
727 Gattass, C. R. Oleanolic acid initiates apoptosis in non-small cell lung cancer cell lines
728 and reduces metastasis of a B16F10 melanoma model in vivo. *PloS one* **2011,** *6*, (12),
729 e28596.
730 38. Yan, S. L.; Huang, C. Y.; Wu, S. T.; Yin, M. C. Oleanolic acid and ursolic acid
731 induce apoptosis in four human liver cancer cell lines. *Toxicology in vitro : an*
732 *international journal published in association with BIBRA* **2010,** *24*, (3), 842-8.
733 39. Cespi, M.; Casettari, L.; Bonacucina, G.; Giorgioni, G.; Perinelli, D. R.; Palmieri, G.
734 F. Evaluation of methoxy polyethylene glycol-polylactide diblock copolymers as
735 additive in hypromellose film coating. *Polym Advan Technol* **2013,** *24*, (11), 1018-1024.
736 40. Perinelli, D. R.; Bonacucina, G.; Cespi, M.; Naylor, A.; Whitaker, M.; Palmieri, G. F.;
737 Giorgioni, G.; Casettari, L. Evaluation of P(L)LA-PEG-P(L)LA as processing aid for
738 biodegradable particles from gas saturated solutions (PGSS) process. *International journal*
739 *of pharmaceutics* **2014,** *468*, (1-2), 250-7.
740 41. Tong, H. H.; Wu, H. B.; Zheng, Y.; Xi, J.; Chow, A. H.; Chan, C. K. Physical
741 characterization of oleanolic acid nonsolvate and solvates prepared by solvent
742 recrystallization. *International journal of pharmaceutics* **2008,** *355*, (1-2), 195-202.

743 42. Danhier, F.; Ansorena, E.; Silva, J. M.; Coco, R.; Le Breton, A.; Preat, V.
744 PLGA-based nanoparticles: an overview of biomedical applications. *Journal of controlled*
745 *release : official journal of the Controlled Release Society* **2012,** *161*, (2), 505-22.
746 43. Venkataraman, S.; Ong, W. L.; Ong, Z. Y.; Joachim Loo, S. C.; Ee, P. L.; Yang, Y. Y.
747 The role of PEG architecture and molecular weight in the gene transfection performance
748 of PEGylated poly(dimethylaminoethyl methacrylate) based cationic polymers.
749 *Biomaterials* **2011,** *32*, (9), 2369-78.
750 44. Owens, D. E., 3rd; Peppas, N. A. Opsonization, biodistribution, and
751 pharmacokinetics of polymeric nanoparticles. *International journal of pharmaceutics*
752 **2006,** *307*, (1), 93-102.
753 45. Li, Y.; Qi, X. R.; Maitani, Y.; Nagai, T. PEG-PLA diblock copolymer micelle-like
754 nanoparticles as all-trans-retinoic acid carrier: in vitro and in vivo characterizations.
755 *Nanotechnology* **2009,** *20*, (5), 055106.
756 46. Liu, Y.; Li, K.; Liu, B.; Feng, S. S. A strategy for precision engineering of
757 nanoparticles of biodegradable copolymers for quantitative control of targeted drug
758 delivery. *Biomaterials* **2010,** *31*, (35), 9145-55.
759 47. Bommana, M. M.; Kirthivasan, B.; Squillante, E. In vivo brain microdialysis to
760 evaluate FITC-dextran encapsulated immunopegylated nanoparticles. *Drug delivery* **2012,**
761 *19*, (6), 298-306.
762 48. Alexis, F.; Pridgen, E.; Molnar, L. K.; Farokhzad, O. C. Factors affecting the
763 clearance and biodistribution of polymeric nanoparticles. *Molecular pharmaceutics* **2008,**
764 *5*, (4), 505-15.
765 49. Hua, M. Y.; Yang, H. W.; Liu, H. L.; Tsai, R. Y.; Pang, S. T.; Chuang, K. L.; Chang, Y.
766 S.; Hwang, T. L.; Chang, Y. H.; Chuang, H. C.; Chuang, C. K. Superhigh-magnetization
767 nanocarrier as a doxorubicin delivery platform for magnetic targeting therapy.

Biomaterials **2011,** *32*, (34), 8999-9010.

50. Vila, A.; Sanchez, A.; Evora, C.; Soriano, I.; McCallion, O.; Alonso, M. J. PLA-PEG particles as nasal protein carriers: the influence of the particle size. *International journal of pharmaceutics* **2005,** *292*, (1-2), 43-52.

51. Essa, S.; Rabanel, J. M.; Hildgen, P. Effect of polyethylene glycol (PEG) chain organization on the physicochemical properties of poly(D, L-lactide) (PLA) based nanoparticles. *European journal of pharmaceutics and biopharmaceutics : official journal of Arbeitsgemeinschaft fur Pharmazeutische Verfahrenstechnik e.V* **2010,** *75*, (2), 96-106.

52. Nduna, M. K.; Lewis, A. E.; Nortier, P. A model for the zeta potential of copper sulphide. *Colloid Surface A* **2014,** *441*, 643-652.

53. Shanmugam, M. K.; Dai, X.; Kumar, A. P.; Tan, B. K.; Sethi, G.; Bishayee, A. Oleanolic acid and its synthetic derivatives for the prevention and therapy of cancer: preclinical and clinical evidence. *Cancer letters* **2014,** *346*, (2), 206-16.

54. Ma, C. M.; Wu, X. H.; Masao, H.; Wang, X. J.; Kano, Y. HCV protease inhibitory, cytotoxic and apoptosis-inducing effects of oleanolic acid derivatives. *Journal of pharmacy & pharmaceutical sciences : a publication of the Canadian Society for Pharmaceutical Sciences, Societe canadienne des sciences pharmaceutiques* **2009,** *12*, (3), 243-8.

55. Kim, S. Y.; Kim, J. H.; Kim, D.; An, J. H.; Lee, D. S.; Kim, S. C. Drug-releasing kinetics of MPEG/PLLA block copolymer micelles with different PLLA block lengths. *J Appl Polym Sci* **2001,** *82*, (10), 2599-2605.

56. Chen, M.; Zhong, Z.; Tan, W.; Wang, S.; Wang, Y. Recent advances in nanoparticle formulation of oleanolic acid. *Chinese medicine* **2011,** *6*, (1), 20.

57. Gao, D.; Tang, S.; Tong, Q. Oleanolic acid liposomes with polyethylene glycol modification: promising antitumor drug delivery. *International journal of nanomedicine*

2012, *7*, 3517-26.

58. Huang, Y.; Li, Y.; Li, X. Z.; Liu, S.; Lei, P.; Xiao, J. Study on the release of oleanolic acid loaded nanocapsules in vitro. *Journal of Chinese Medicinal Materials* **2008,** *31*, (2), 283-5.

59. Garofalo, C.; Capuano, G.; Sottile, R.; Tallerico, R.; Adami, R.; Reverchon, E.; Carbone, E.; Izzo, L.; Pappalardo, D. Different insight into amphiphilic PEG-PLA copolymers: influence of macromolecular architecture on the micelle formation and cellular uptake. *Biomacromolecules* **2014,** *15*, (1), 403-15.

60. Li, H.; He, N.; Li, X.; Zhou, L.; Zhao, M.; Jiang, H.; Zhang, X. Oleanolic acid inhibits proliferation and induces apoptosis in NB4 cells by targeting PML/RARalpha. *Oncology letters* **2013,** *6*, (4), 885-890.